Zheng, D., Chang, S.-C., Ramezani, J., Xu, X., Xu, H., Wang, H., Pei, R., Fang, Y., Wang, J., Wang, B., and Zhang, H., 2023, Calibrating Early Cretaceous Urho Pterosaur Fauna in the Junggar Basin and implications for the evolution of the Jehol Biota: GSA Bulletin, https://doi.org/10.1130/B36795.1.

Supplemental Material

Supplemental Text S1. Stratigraphic information, U-Pb geochronology by LA-MC-ICP-MS, and U-Pb geochronology by CA-ID-TIMS.

Figure S1. Cathodoluminescent images of zircons from sample W-1 with youngest ages analyzed by LA-MC-ICP-MS U-Pb dating.

Figure S2. Rank order plot of LA-MC-ICP-MS U-Pb ages for youngest zircon subpopulations from sample W-1.

Table S1. Vertebrate and trace fossils from the Tugulu Group of the Junggar Basin.

Table S2. LA-MC-ICP-MS U-Pb analytical results for standard zircons and sample W-1.

Table S3. CA-ID-TIMS U-Pb analytical results for sample W-1.

Supplemental Text S1

Stratigraphic information

Abundant fossils, especially belonging to vertebrates, have been reported from the Tugulu Group (Table S1). These include diverse pterosaur, plesiosaur, dinosaur, crocodylomorph, fish, turtle, conchostracan, bivalve, ostracod, charophyte, and sporopollen fossils. In the southern Junggar Basin, the Tugulu Group consists of the Qingshuihe, Hutubihe, Shengjinkou, and Lianmuqin formations. The Qingshuihe Formation is absent in the NW Junggar Basin (Zhao, 1980).

In Urho, the Hutubihe Formation unconformably overlies a thick Devonian conglomerate, reaches 150 m thickness, and consists primarily of grey-green, grey-yellow conglomerate, sandstone, and red-brown, grey-green mudstone. Mudstone in the lower Hutubihe Formation hosts vertebrate fossils including material from pterosaurs, plesiosaurs, crocodylomorphs, and dinosaurs. These fossils however have not been systematically interpreted (Zhao, 1980). Hundreds of bird, theropod, stegosaur, pterosaur, and turtle tracks also occur in upper layers of this formation.

The Shengjinkou Formation conformably overlies the Hutubihe Formation and conformably underlies the Lianmuqin Formation. It consists of a series of thick, grey-green, grey-yellow sandstones interbedded with mudstone and reaching a cumulative thickness of ca. 250 m. The lowermost Shengjinkou Formation includes a yellow conglomerate that grades into an uppermost white tuffaceous siltstone (0.2 m thick). Vertebrate fossils occur in the grey-green mudstone. These belong to the pterosaurs *Dsungaripterus weii* and *Noripterus complicidens* and the dinosaur Camarasauridae indet. (Young, 1973; Zhao, 1980; Wings et al., 2010).

The Lianmuqin Formation unconformably underlies the Upper Cretaceous Ailike Formation. The Lianmuqin Formation consists primarily of grey-green sandstone, grey-yellow sandy mudstone, and red-brown mudstone reaching a cumulative thickness of ca. 430 m. Vertebrate fossils in the sandstone and mudstone include the pterosaurs *Dsungaripterus weii*, *Noripterus complicidens*, the plesiosaur *Sinopliosaurus weiyuanensis*, turtles *Xinjiangchelys* sp., *Ordosemys brinkmania*, and cf. Pantrionychia, the crocodylomorph *Edentosuchus tienshanensis*, and the dinosaurs *Tugulusaurus faciles*, *Phaedrolosaurus ilikensis*, *Xinjiangovenator parvus*, *Kelmayisaurus petrolicus*, cf. *Asiatosaurus mongoliensis*, *Psittacosaurus xinjiangensis*, and *Wuerhosaurus homheni* (Young, 1964, 1973; Dong,1973; Li, 1985; Brinkman et al., 2001; Pol et al., 2004; Rauhut and Xu, 2005; Danilov and Parham, 2007; Wings et al., 2010).

At the Jiamuhe section an isolated, white, tuffaceous horizon occurs at the boundary between the Shengjinkou and Lianmuqin formations (Figs. 2C, 3 and 5). The tuffaceous marker bed is approximately 20 cm thick, is laterally continuous in the outcrop and exhibits sharp contacts with the enclosing sandstones and siltstones. It locally diverges into separate, closely spaced tuffaceous layers interbedded with the latter lithologies (Fig. 3). The tuffaceous siltstone is soft, clay-rich and friable when dry.

U-Pb geochronology by LA-MC-ICP-MS

The tuffaceous sample W-1 from the Jiamuhe section was mechanically crushed and underwent mineral separation using standard sieving, magnetic, and high-density liquid techniques. Zircons were then manually selected using a binocular microscope. One hundred small, inclusion-free, zircon grains (40–70 μm in length) from the sample were mounted in epoxy resin. Hardened mounts were polished to expose zircon grain midsections to about one-half of their width. Cathodoluminescence (CL) imaging was used to document grain morphologies and internal structure for *in situ* analysis (fig. S2). U-Pb isotopic data on zircons were measured at the Department of Earth Sciences, University of Hong Kong, using a Nu Instruments Multi-Collector (MC) ICP-MS with a Resonetics RESOlution M-50-HR Excimer Laser Ablation System. The analyses used a beam diameter of 30 μm, repetition rate of 4 Hz, and energy density of 5 J/cm^2 on the sample surface. The average ablation time was approximately 25 s, and pit depths reached about 20 to 30 μm. The standard zircons 91500 (Wiedenbeck, 1995) and GJ-1 (Jackson et al., 2004) were used for data validation. The zircon 91500 was used as an external calibration standard to evaluate the magnitude of mass bias and inter-elemental fractionation. The zircon GJ-1 was used to evaluate the accuracy and reproducibility of the laser ablation results. The software ICPMSDataCal Version 8.0 (Liu et al., 2010) was used to process the off-line signal selection, quantitative calibration, and time-drift correction. We used a function given in Anderson (Anderson, 2002) to correct for common Pb in Microsoft Excel. Concordant and rank order plots were created using ISOPLOT/Excel version 3.0 (Ludwig, 2003).

In this study, 20 zircon grains were randomly selected from the sample so that the results would capture the overall character of the age populations. $^{206}Pb/^{238}U$ ages were interpreted for zircon grains younger than 1000 Ma, and $^{207}Pb/^{206}Pb$ ages were interpreted for older grains. Ages were retained only for analyses exhibiting concordance of 95% or more and after excluding distinguishably older (detrital) analyses. Table S1 lists U-Pb data results. Average 2σ analytical uncertainty was ± 1.6 myr for the analyzed zircons of

Cretaceous age. The sample age is derived from the weighted mean $^{206}Pb/^{238}U$ date of nine youngest analyses with its 95% confidence level uncertainty reported using ± α/β Ma notation, where α is the internal (analytical) uncertainty in the absence of all external errors, and β incorporates α as well as the external reproducibility (age bias). β must be taken into account when comparing U-Pb ages measured by different analytical techniques (e.g., *in situ* dating versus ID-TIMS). Analysis of the 6 secondary standard GJ-1 in the present study provides an age of 601.6 ± 1.9 Ma. Considering that the accepted age for GJ-1 (Hortswood et al. 2016) is 601.95 ± 0.40 Ma, our analyses are off target by 0.25%. 0.25% of 135.2 Ma is 0.34 m.y. Then we can calculate the β error: SQRT ((0.5^2) + (0.34^2)) = 0.6 m.y.

U-Pb geochronology by CA-ID-TIMS

A set of zircons from sample W-1 were analyzed by the high-precision CA-ID-TIMS method following the procedures described in Ramezani et al. (2022). Zircons were pre-treated using a chemical abrasion technique modified after Mattinson (2005). This involved thermal annealing in a furnace at 900°C for 60 hours, followed by partial dissolution in 29 M HF at 210°C in high-pressure vessels for 12 hours. This procedure mitigates the effects of radiation-induced Pb loss in zircon and thus improves the accuracy of U-Pb dates. (Removal of Pb-loss areas is not possible with *in situ* dating techniques.) The chemically abraded grains were successively fluxed in several hundred microliters of dilute HNO_3 and 6M HCl on a hot plate and in an ultrasonic bath (1 hour each). Material was rinsed with several volumes of Millipore water in between fluxes to remove the leachates.

Pretreated zircon grains were spiked with a mixed ^{205}Pb-^{233}U-^{235}U isotopic tracer (ET535; Condon et al., 2015; McLean et al., 2015) prior to complete dissolution in 29 M HF at 210°C for 48 hours and subsequent Pb and U purification via an HCl-based anion-exchange column chemistry (Krogh, 1973). Purified Pb and U were loaded together onto single outgassed Re filaments along with a silica-gel emitter solution. Their isotopic ratios were measured using an Isotopx X62 multi-collector thermal ionization mass spectrometer equipped with a Daly photomultiplier ion-counting system at the Massachusetts Institute of Technology Isotope Laboratory. Pb isotopes were measured as mono-atomic ions in peak-hopping mode on the ion-counter and were corrected for a mass-dependent isotope fractionation of 0.18% ± 0.05% per atomic mass unit (2σ). U isotopes were measured as dioxide ions in static mode using three Faraday collectors. Ratios were subjected to an oxide correction using an independently determined $^{18}O/^{16}O$ ratio of 0.00205 ± 0.00005. Within-run U mass fractionation corrections were made using the $^{233}U/^{235}U$ ratio of the tracer and a predicted sample $^{238}U/^{235}U$ ratio of 137.818 ± 0.045 (Hiess et al., 2012).

A total of 5 zircons from sample W-1 were analysed by the CA-ID-TIMS method. Table S2 lists complete Pb and U isotopic data and Figure 3b shows age results as ranked age plots. Data reduction, calculation of dates, and propagation of uncertainties used the Tripoli and ET_Redux applications and algorithms (Bowring et al., 2011; McLean et al., 2011). The individual $^{206}Pb/^{238}U$ dates were corrected for initial ^{230}Th disequilibrium based on an assumed magma Th/U ratio of 2.8 ± 1.0 (2σ). The 2σ analytical uncertainty of individual zircon dates ranged from ± 0.34 myr to ± 0.92 myr. The relatively high uncertainty of the CA-ID-TIMS method here is due to the small zircon size and thus small amounts of measured radiogenic Pb (<2.5 pg) and U (<100 pg).

References cited

Augustin, F.J., Matzke, A.T., Maisch, M.W., and Pfretzschner, H.-U., 2021, New information on *Lonchognathosaurus* (Pterosauria: Dsungaripteridae) from the Lower Cretaceous of the southern Junggar Basin (NW China): Cretaceous Research, v. 124, p.104808, https://doi.org/10.1016/j.cretres.2021.104808.

Augustin, F.J., Matzke, A.T., Maisch, M.W., and Csiki-Sava, Z., 2022a, Pterosaur remains from the Lower Cretaceous Lianmuxin Formation (upper Tugulu Group) of the southern Junggar Basin (NW China): Historical Biology, v. 34, p. 312–321, DOI: 10.1080/08912963.2021.1910819.

Augustin, F.J., Matzke, A.T., Maisch, M.W., Kampouridis, P., and Csiki-Sava, Z., 2022b, The first record of pterosaurs from the Lower Cretaceous Hutubei Formation (lower Tugulu Group) of the southern Junggar Basin (NW China)–A glimpse into an unusual ecosystem: Cretaceous Research, v. 130, p. 105066, https://doi.org/10.1016/j.cretres.2021.105066.

Anderson, T., 2002, Correction of common lead in U–Pb analyses that do not report ^{204}Pb: Chemical Geology, v. 192, p. 59–79, https://doi.org/10.1016/S0009-2541(02)00195-X.

Bowring, J.F., McLean, N.M., Bowring, S.A., 2011. Engineering cyber infrastructure for U-Pb geochronology: Tripoli and U-Pb_Redux. Geochem. Geophy. Geosy. 12, Q0AA19. DOI:10.1029/2010GC003478.

Brinkman, D.B., Eberth, D.A., Ryan, M.J., and Chen, P., 2001, The occurrence of *Psittacosaurus xinjiangensis* Sereno and Chow, 1988 in the Urho area, Junggar Basin, Xinjiang, People's Republic of China, *in* Currie, P., ed., The Sino-Canadian Dinosaur Project 3: Canadian Journal of Earth Sciences, v. 38, p. 1781–1786.

Condon, D.J., Schoene, B., McLean, N.M., Bowring, S.A., Parrish, R.R., 2015. Metrology and traceability of U-Pb isotope dilution geochronology (EARTHTIME Tracer Calibration Part I). Geochim. Cosmochim. Ac. 164, 464–480. https://doi.org/10.1016/j.gca.2015.05.026.

Danilov, I.G., and Parham, J.F., 2007, The type series of '*Sinemys*' *wuerhoensis*, a problematic turtle from the Lower Cretaceous of China, includes at least three taxa: Palaeontology, v. 50, p. 431–444, doi:10.1111/j.1475-4983.2006.00632.x.

Dong, Z., 1973, Dinosaurs from Wuerho: Memoirs of the Institute of Vertebrate Paleontology and Paleoanthropolgy, Academia Sinica, v. 11, p. 45–52.

He, Q., Xing, L., Zhang, J., Lockley, M.G., Klein, H., Persons IV, W.S., Qi, L., and Jia, C., 2013, New Early Cretaceous pterosaur–bird track assemblage from Xinjiang, China: palaeoethology and paleoenvironment: Acta Geologica Sinica, v. 87, p. 1477–1485, https://doi.org/10.1111/1755-6724.12151.

Hiess, J., Condon, D.J., McLean, N., Noble, S.R., 2012. $^{238}U/^{235}U$ Systematics in Terrestrial Uranium-Bearing Minerals. Science 335, 1610–1614. DOI: 10.1126/science.1215507.

Hone, D.W.E., Jiang, S., Xu, X., 2018. A taxonomic revision of *Noripterus complicidens* and Asian members of the Dsungaripteridae. Geol. Soc. Spec. Publ. 455, 149–157. https://doi.org/10.1144/SP455.8.

Horstwood, M.S.A., et al., 2016. Community-derived standards for LA-ICP-MS U-(Th-) Pb geochronology - uncertainty propagation, age Interpretation and data reporting. Geostand. Geoanal. Res. 40, 311–332. https://doi.org/10.1111/j.1751-908X.2016.00379.x.

Jackson, S.E., Pearson, N.J., Griffin, W.L., and Belousova, E.A., 2004, The application of laser ablation-inductively coupled plasma-mass spectrometry to in situ U–Pb zircon geochronology: Chemical Geology, v. 211, p. 47–69, https://doi.org/10.1016/j.chemgeo.2004.06.017.

Khosatzky, L.I., 1996, New turtle from the Early Cretaceous of Central Asia: Russian Journal of Herpetology, v. 3, p. 89–94.

Krogh, T.E., 1973. Low-Contamination Method for Hydrothermal Decomposition of Zircon and Extraction of U and Pb for Isotopic Age Determinations. Geochim. Cosmochim. Ac. 37, 485–494. https://doi.org/10.1016/0016-7037(73)90213-5.

Li, D., and Ji, S., 2010, New Material of the Early Cretaceous pterosaur *Dsungaripterus Weii* from northern Xinjiang, Northwest China: Acta Geoscientica Sinica, v. 31, p. 38–39.

Li, J., 1985, A revision of *Edentosuchus tienshanensis* Young from the Tugulu Group of Xingjiang Autonomous Region: Vertebrata Palasiatica, v. 23, p. 196–206

Li, Y., Jiang, S., Wang, X., 2020. The largest species of *Asianopodus* footprints from Junggar Basin, Xinjiang, China (in Chinese). Chin. Sci. Bull. 65, 1875–1887. DOI: 10.1360/TB-2019-0513.

Liu, Y., Gao, S., Hu, Z., Gao, C., Zong, K., Wang, D., 2010. Continental and oceanic crust recycling-induced melt-peridotite interactions in the trans-north China

orogen: U–Pb dating, Hf isotopes and trace elements in zircons from mantle xenoliths. J. Petrol. 51, 537–571.
Ludwig, K.R., 2003, Isoplot v. 3.0: A geochronological toolkit for Microsoft excel: Special Publication, No. 4. Berkeley Geochronology Center, 70 p.
Maisch, M., Matzke, A., and Sun, G., 2003, A new sinemydid turtle (Reptilia: Testudines) from the Lower Cretaceous of the Junggar Basin (NW China): Neues Jahrbuch für Geologie und Paläontologie Monatshefte, v. 12, p. 705–722.
Maisch, M.W., Matzke, A.T., and Sun, G., 2004, A new dsungaripteroid pterosaur from the Lower Cretaceous of the southern Junggar Basin, north-west China: Cretaceous Research, v. 25, p. 625–634, doi:10.1007/s12549-010-0031-3.
Mattinson, J.M., 2005. Zircon U/Pb chemical abrasion (CA-TIMS) method; combined annealing and multi-step partial dissolution analysis for improved precision and accuracy of zircon ages. Chem. Geol. 220, 47–66. https://doi.org/10.1016/j.chemgeo.2005.03.011.
Matzke, A.T., and Maisch, M.W., 2004, New information and specimens of *Wuguia hutubeiensis* (Reptilia: Testudines) from the Lower Cretaceous Tugulu Group of the southern Junggar Basin (NW China): Neues Jahrbuch für Geologie und Paläontologie Monatshefte, v. 8, p. 473–495.
McLean, N.M., Bowring, J.F., Bowring, S.A., 2011. An algorithm for U-Pb isotope dilution data reduction and uncertainty propagation. Geochem. Geophy. Geosy. 12, Q0AA18. DOI:10.1029/2010GC003479.
McLean, N.M., Condon, D.J., Schoene, B., Bowring, S.A., 2015. Evaluating uncertainties in the calibration of isotopic reference materials and multi-element isotopic

tracers (EARTHTIME Tracer Calibration Part II). Geochim. Cosmochim. Ac. 164, 481–501. https://doi.org/10.1016/j.gca.2015.02.040.

Pol, D., Ji, S., Clark, J.M., and Chiappe, L.M., 2004, Basal crocodyliforms from the Lower Cretaceous Tugulu Group (Xinjiang, China), and the phylogenetic position of Edentosuchus: Cretaceous Research, v. 25, p. 603–622, https://doi.org/10.1016/j.cretres.2004.05.002.

Ramezani, J., Beveridge, T. L., Rogers, R. R., Eberth, D. A., and Roberts, E. M., 2022, Calibrating the zenith of dinosaur diversity in the Campanian of the Western Interior Basin by CA-ID-TIMS U–Pb geochronology: Scientific Reports, v. 12, no. 1, p. 16026, https://doi.org/ 10.1038/s41598-022-19896-w.

Rauhut, O.W.M., and Xu, X., 2005, The small theropod dinosaurs Tugulusaurus and Phaedrolosaurus from the Early Cretaceous of Xinjiang, China: Journal of Vertebrate Paleontology, v. 25, p. 107–118, https://doi.org/10.1671/0272-4634(2005)025[0107:TSTDTA]2.0.CO;2.

Sereno, P.C., and Chao, S., 1988, *Psittacosaurus xinjiangensis* (Ornithischia: Ceratopsia), a new psittacosaur from the Lower Cretaceous of northwestern China: Journal of Vertebrate Paleontology, v. 8, p. 353–365, https://doi.org/10.1080/02724634.1988.10011724.

Su, D., 1980, On late Mesozoic fish fauna from Sinjiang, China: Vertebrata PalAsiatica, v. 18, p. 76–80.

Su, D., 1985, On late Mesozoic fish fauna from Xinjiang (Sinkiang), China: Memoirs of Institute of Vertebrate Palaeontology and Palaeoanthropology, Academia Sinica, v.

17, p. 61–136.

Wiedenbeck, M., Alle, P., Corfu, F., Griffin, W.L., Meier, M., Oberli, F., Quadt, A., Roddick, J.C., and Spiegel, W., 1995, Three natural zircon standards for U–Th–Pb, Lu–Hf, trace element and REE analyses: Geostandards and Geoanalytical Research, v. 19, p. 1–23, https://doi.org/10.1111/j.1751-908X.1995.tb00147.x.

Wings, O., Schwarz-Wings, D., Pfretzschner, H.U., and Martin, T., 2010, Overview of Mesozoic crocodylomorphs from the Junggar Basin, Xinjiang, northwest China and description of isolated crocodyliform teeth from the Late Jurassic Liuhuanggou locality, *in* Martin, T., Sun, G., Mosbrugger, V., eds., Triassic–Jurassic Biodiversity, Ecosystems, and Climate in the Junggar Basin, Xinjiang, northwest China: Palaeobiodiversity and Palaeoenvironments, v. 90, p. 283–294, doi:10.1007/s12549-010-0033-1.

Xing, L., Avanzini, M., Lockley, M.G., Miyashita, T., Klein, H., Zhang, J., He, Q., QI, L., Divay, J.D., and Jia, C., 2014, Early Cretaceous turtle tracks and skeletons from the Junggar Basin, Xinjiang, China: PALAIOS, v. 29, p. 137–144, https://doi.org/10.2110/palo.2014.012.

Xing, L., Harris, J.D., Jia, C., Luo, Z., Wang, S., and An, J., 2011, Early Cretaceous bird-dominated and dinosaur footprint assemblages from the northwestern margin of the Junggar Basin, Xinjiang, China: Palaeoworld, v. 20, p. 308–321, https://doi.org/10.1016/j.palwor.2011.01.001.

Xing, L., Lockley, M.G., Klein, H., Zhang, J., He, Q., Divay, J.D., Qi, L., and Jia, C., 2013a, Dinosaur, bird and pterosaur footprints from the Lower Cretaceous of Wuerhe asphaltite area, Xinjiang, China, with notes on overlapping track relationships: Palaeoworld, v. 22, p. 42–51, https://doi.org/10.1016/j.palwor.2013.03.001.

Xing, L., Lockley, M.G., Mccrea, R.T., Gierliński, G.D., Buckley, L.G., Zhang, J., Qi, L., and Jia, C., 2013b, First record of *Deltapodus* tracks from the Early Cretaceous of China: Cretaceous Research, v. 42, p. 55–65, https://doi.org/10.1016/j.cretres.2013.01.006.

Yeh, X.-K., 1973, Chelonia fossils from Wuerho: Memoir of the Institute of Vertebrate Palaeontology and Paleoanthropology, Academia Sinica, v. 11, p. 8–12.

Young, C.-C., 1964, On a new pterosaurian from Sinkiang: Vertebrate PalAsiatica, v. 8, p. 221–225.

Young, C.-C., 1973, Pterosaurian Fauna from Wuerho, Sinkiang: Memoir of the Institute of Vertebrate Palaeontology and Paleoanthropology, Academia Sinica, v. 11, p. 18–35.

Zhao, X., 1980, The Mesozoic vertebrate Fossils and Stratigraphy in northern Xinjiang: Science Press, Beijing, 120 p.

Figure S1. Cathodoluminescent images of zircons from sample W-1 with youngest ages analyzed by LA-MC-ICP-MS U-Pb dating. Age uncertainties are given at the 1σ level.

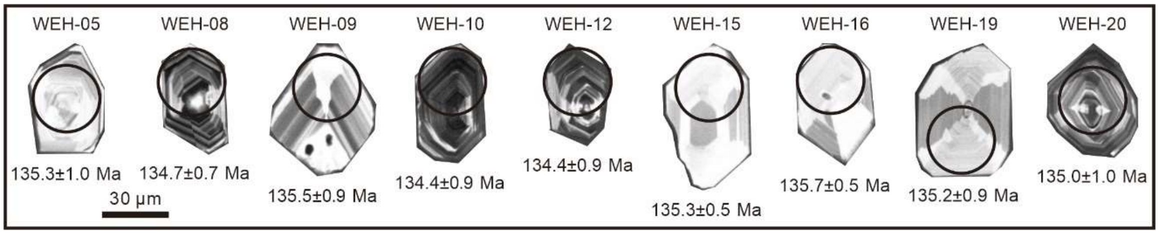

Figure S2. Rank order plot of LA-MC-ICP-MS U-Pb ages for youngest zircon subpopulations from sample W-1. Horizontal lines in rank order plot signify calculated sample dates. The width of the shaded band represents internal uncertainty in the weighted mean age at a 95% confidence level. Age uncertainties are given at the 2σ level. MSWD—mean square of weighted deviates.

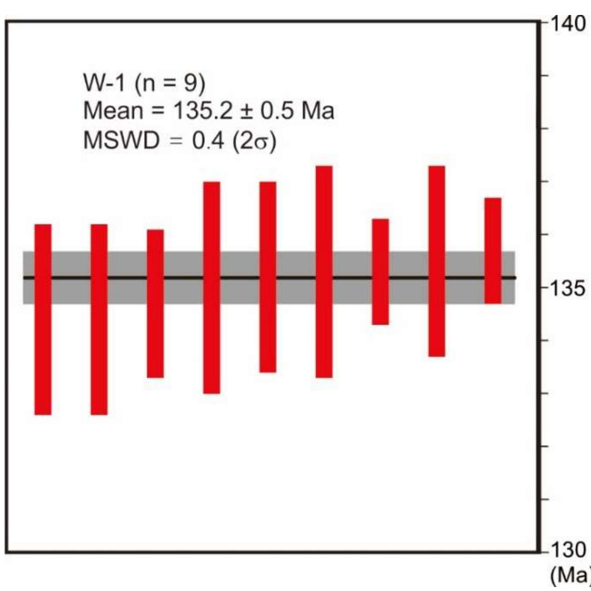

Table S1. Vertebrate and trace fossils from the Tugulu Group of the Junggar Basin. Numbers correspond references: [1] Young (1964); [2] Young (1973); [3] Yeh (1973), Danilov and Parham (2007); [4] Dong (1973); [5] Sereno and Chao (1988); [6] Young (1973), Li (1985), Pol et al. (2004), Wings et al. (2004); [7] Zhao (1980); [8] Xing et al. (2011); [9] Xing et al. (2013a), He et al. (2013); [10] Xing et al. (2014); [11] Xing et al. (2011), Xing et al. (2013a); [12] Xing et al. (2013b); [13] Maisch et al. (2004), Augustin et al. (2021); [14] Augustin et al. (2022a); [15] Brinkman (2001); [16] Maisch et al. (2003), Danilov and Sukhanov (2006); [17] Su (1980, 1985); [18] Augustin et al. (2022b); [19] Matzke and Maisch (2004); [20] Khosatzky (1996).

		NW Junggar Basin	Southern Junggar Basin
Tugulu Group	Lianmuqin Fm.	pterosaur: *Dsungaripterus weii* [1] *Noripterus complicidens* [2] turtle: *Xinjiangchelys* sp. [3] *Ordosemys brinkmania* [3] cf. Pantrionychia indet. [3] dinosaur: *Tugulusaurus faciles* [4] *Xinjiangovenator parvus* [5] *Kelmayisaurus petrolicus* [4] cf. *Asiatosaurus mongoliensis* [4] *Psittacosaurus xinjiangensis* [5] *Wuerhosaurus homheni* [4] plesiosaur *Sinopliosaurus weiyuanensis* [2] crurotarsan: *Edentosuchus tienshanensis* [6]	pterosaur: *Lonchognathosaurus acutirostris* [13] Dsungaripteridae indet. [14] turtle: *Dracochelys bicuspis* [15] *Wuguia efremovi* [16]

	Shengjinkou Fm.	pterosaur: *Dsungaripterus weii* [7] *Noripterus complicidens* [7] dinosaur: Camarasauridae indet. [7]	fish: *Uighuroniscus sinkiangensi* [17] *Manasichthys tuguluensis* [17] *Dsungarichthys bilineatus* [17] *Manasichthys elongates* [17] *Bogdaichthys fukangensis* [17] *Bogdaichthys serratus* [17]
	Hutubihe Fm.	bird tracks: *Koreanaornis dodsoni* [8] *Goseongornipes* isp. [8] *Aquatilavipes* isp. [8] *Moguiornipes robusta* [8] pterosaur tracks: *Pteraichnus* isp. [9] turtle tracks: *Chelonipus* isp. [10] *Emydhipus* isp. [10] Non-avian theropod tracks: cf. *Jialingpus* isp. [11] *Asianopodus* isp. [8] *Kayentapus* isp. [8] *Deltapodus curriei* [12]	pterosaur: Dsungaripteridae indet. [18] turtle: *Wuguia efremovi* [19] *Wuguia hutubeiensis* [20]
	Qingshuihe Fm.		

Table S2. LA-MC-ICP-MS U-Pb analytical results for standard zircons and sample W-1.

Samples	Isotopic ratios							rho	U-Pb Ages (Ma)						discor.
	Th/U	$^{207}Pb/^{206}Pb$	±1σ	$^{207}Pb/^{235}U$	±1σ	$^{206}Pb/^{238}U$	±1σ		$^{207}Pb/^{206}Pb$	±1σ	$^{207}Pb/^{235}U$	±1σ	$^{206}Pb/^{238}U$	±1σ	
Standard samples															
91500std	0.345	0.07463	0.00046	1.8446	0.01306	0.1793	0.00083	0.6526	1059	7	1061	5	1063	5	0
91500std	0.345	0.07463	0.00046	1.8446	0.01306	0.1793	0.00083	0.6526	1059	7	1061	5	1063	5	0
91500std	0.35	0.07513	0.00059	1.8558	0.01647	0.1791	0.00079	0.498	1072	11	1065	6	1062	4	0
91500std	0.356	0.07509	0.00043	1.8551	0.0117	0.1791	0.00084	0.7465	1071	6	1065	4	1062	5	0
91500std	0.338	0.07467	0.00044	1.8453	0.01347	0.1792	0.00094	0.7183	1060	7	1062	5	1063	5	0
91500std	0.35	0.07488	0.00048	1.8525	0.014	0.1793	0.00076	0.5638	1065	9	1064	5	1063	4	0
91500std	0.345	0.07488	0.00047	1.848	0.01202	0.179	0.00077	0.6637	1065	7	1063	4	1062	4	0
GJ-1	0.028	0.06023	0.00035	0.8123	0.00548	0.0978	0.00039	0.5857	612	8	604	3	601	2	0
GJ-1	0.028	0.0604	0.00033	0.8151	0.00556	0.0978	0.00042	0.6275	618	8	605	3	602	2	0
GJ-1	0.028	0.05995	0.00029	0.8087	0.00546	0.0978	0.00051	0.7791	602	7	602	3	601	3	0
GJ-1	0.028	0.06022	0.00025	0.8124	0.00476	0.0978	0.00048	0.8314	612	6	604	3	601	3	0
GJ-1	0.027	0.06046	0.00028	0.8169	0.00463	0.098	0.00038	0.6818	620	6	606	3	602	2	1
GJ-1	0.028	0.06042	0.00033	0.8151	0.00475	0.0978	0.00045	0.7884	619	6	605	3	602	3	0
W-01	0.592	0.05651	0.00024	0.6035	0.00569	0.0774	0.00067	0.9238	472	9	479	4	481	4	0
W-02	1.163	0.05238	0.00041	0.373	0.00498	0.0516	0.00052	0.7574	302	14	322	4	324	3	1
W-03	0.704	0.05209	0.0006	0.1519	0.00234	0.0211	0.00011	0.3421	289	25	144	2	134.9	0.7	7
W-04	0.862	0.0652	0.0004	1.1285	0.008	0.1255	0.00053	0.5946	781	8	767	4	762	3	1
W-05	0.68	0.05053	0.00049	0.1479	0.00172	0.0212	0.00015	0.6215	220	14	140	2	135.3	1	3
W-06	0.901	0.05513	0.00528	0.162	0.01548	0.0213	0.00015	0.2749	418	219	152	14	135.9	1	12
W-07	1.266	0.05442	0.00047	0.3317	0.00452	0.0441	0.0003	0.5065	388	18	291	3	278	2	5
W-08	0.99	0.05055	0.00125	0.1472	0.00355	0.0211	0.00011	0.6625	220	58	139	3	134.7	0.7	3
W-09	0.84	0.04914	0.00054	0.1441	0.00176	0.0213	0.00014	0.5547	155	16	137	2	135.5	0.9	1
W-10	0.446	0.04974	0.00149	0.1445	0.0042	0.0211	0.00015	0.4875	183	71	137	4	134.4	0.9	2
W-11	0.595	0.05311	0.00097	0.164	0.00289	0.0224	0.00011	0.6799	333	42	154	3	142.8	0.7	8
W-12	0.415	0.05126	0.00187	0.1489	0.00534	0.0211	0.00015	0.3858	252	86	141	5	134.4	0.9	5
W-13	0.571	0.05184	0.00078	0.1658	0.00223	0.0232	0.00015	0.859	278	35	156	2	147.8	1	6
W-14	1.042	0.05803	0.00073	0.552	0.00612	0.069	0.0004	0.9846	531	28	446	4	430	2	4
W-15	0.337	0.05067	0.0008	0.1482	0.00231	0.0212	0.00009	0.2609	226	28	140	2	135.3	0.5	3

W-16	1.205	0.05023	0.00053	0.1473	0.00151	0.0213	0.00007	0.3375	206	17	140	1	135.7	0.5	3
W-17	0.962	0.05233	0.00044	0.1527	0.00141	0.0212	0.00011	0.5771	300	12	144	1	135	0.7	7
W-18	0.562	0.05363	0.00446	0.1531	0.01266	0.0207	0.00018	0.1703	356	191	145	11	132	1	10
W-19	0.84	0.04924	0.00061	0.144	0.00206	0.0212	0.00015	0.4955	159	20	137	2	135.2	0.9	1
W-20	0.87	0.05046	0.00043	0.1478	0.00179	0.0212	0.00018	0.6822	216	14	140	2	135	1	4

Table S3. CA-ID-TIMS U-Pb analytical results for sample W-1. Zircon number in bold indicates analysis providing maximum depositional age.

					Ratios								Ages (Ma)						
Sample Fractions	Pb(c) (pg)	$\frac{Pb^*}{Pb_c}$	U (pg)	$\frac{Th}{U}$	$\frac{^{206}Pb}{^{204}Pb}$	$\frac{^{208}Pb}{^{206}Pb}$	$\frac{^{206}Pb}{^{238}U}$	err	$\frac{^{207}Pb}{^{235}U}$	err	$\frac{^{207}Pb}{^{206}Pb}$	err	$\frac{^{206}Pb}{^{238}U}$	err	$\frac{^{207}Pb}{^{235}U}$	err	$\frac{^{207}Pb}{^{206}Pb}$	err	corr. coef.
(a)	(b)		(c)		(d)	(e)	(f)	(2σ%)	(f)	(2σ%)	(f)	(2σ%)		(2σ)		(2σ)		(2σ)	
z3	0.27	3.3	32	1.17	184.9	0.371	0.022194	(.62)	0.15659	(7.40)	0.05119	(7.20)	141.51	0.87	148	10	248	166	0.35
z4	0.47	3.4	71	0.45	224.1	0.143	0.021722	(.48)	0.15231	(5.79)	0.05088	(5.65)	138.53	0.66	143.9	7.8	234	130	0.34
z5	0.45	2.7	51	0.77	170.2	0.243	0.021535	(.64)	0.15509	(7.64)	0.05226	(7.45)	137.35	0.88	146	10	296	170	0.35
z1	0.29	7.9	94	0.90	445.4	0.285	0.021395	(.25)	0.14625	(2.98)	0.04960	(2.90)	136.47	0.34	138.6	3.9	175	68	0.35
z2	0.37	3.1	48	0.83	190.1	0.264	0.021196	(.69)	0.14622	(8.24)	0.05006	(7.95)	**135.21**	**0.92**	139	11	197	185	0.47

Notes:

(a) Thermally annealed and pre-treated single zircon.

(b) Total common-Pb in analyses.

(c) Total sample U content.

(d) Measured ratio corrected for spike and fractionation only.

(e) Radiogenic Pb ratio.

(f) Corrected for fractionation, spike, and blank. Also corrected for initial Th/U disequilibrium using radiogenic ^{208}Pb and Th/U_{magma} = 2.8.

Mass fractionation correction of 0.18% amu^{-1} ± 0.04% amu^{-1} (atomic mass unit) was applied to single-collector Daly analyses.

All common Pb assumed to be laboratory blank. Total procedural blank less than 0.1 pg for U.

Blank isotopic composition: $^{206}Pb/^{204}Pb = 18.15 \pm 0.47$, $^{207}Pb/^{204}Pb = 15.30 \pm 0.30$, $^{208}Pb/^{204}Pb = 37.11 \pm 0.87$.

Corr. coef. = correlation coefficient.

Ages calculated using the decay constants λ_{238} = 1.55125E-10 and λ_{235} = 9.8485E-10.